



ARCHIVES  
of  
FOUNDRY ENGINEERING

ISSN (2299-2944)  
Volume 2022  
Issue 3/2022

19 – 24

3/3

10.24425/afe.2022.140232



Published quarterly as the organ of the Foundry Commission of the Polish Academy of Sciences

# Inoculation of Gray Cast Iron Intended for Large Scale and Heavy Weight Castings of Bottom Plates and Counterweights Manufactured in the Krakodlew S.A.

A. Szczęsny \* , D. Kopyciński , E. Guzik 

AGH University of Science and Technology,

Faculty of Foundry Engineering, ul. Reymonta 23, 30-059 Kraków, Poland

\* Corresponding author. E-mail address: ascn@agh.edu.pl

Received 06.04.2022; accepted in revised form 03.06.2022; available online 10.07.2022

## Abstract

The paper presents research carried out during the development of new technology for the production of heavy-weight castings of counterweights. The research concerns the procedure of inoculation gray cast iron with flake graphite and indicates guidelines for the development of new technology for obtaining inoculated cast iron for industrial conditions.

The research was conducted in order to verify the possibility of producing large size or heavy-weight castings of plates in a vertical arrangement. The aim is to evenly distribute graphite in the structure of cast iron and thus reduce the volumetric fraction of type D graphite. The tests were carried out using the ProCast program, which was used to determine the reference chemical composition, and the inoculation procedure was carried out with the use of three different inoculants. The work was carried out in project no. RPMP.01.02.01-12-0055 / 18 under the Regional Operational Program of the Lesser Poland Voivodeship in Krakow (Poland).

**Keywords:** Heavy castings, Large scale casting, Grey cast iron, Inoculation

## 1. Introduction

The castings of bottom plates (Fig. 1a) and counterweights (Fig. 1b) belong to the group of large-size and heavy-weight castings. The material used for this type of castings must meet several important conditions. The microstructure in large size castings, shaped during crystallization and cooling, differs significantly from normal size castings, which is associated with such phenomena as element segregation, graphite flotation, a variable proportion of perlite and ferrite, or shrinkage porosity [1,2]. This also applies to steel castings [3-8] and other groups of

materials such as alloy cast iron [9,10] or castings from the group of large-size structures used, for example, in the power industry. Generally, the control of the structure, and in particular the properties of graphite (for grey cast iron), may, to a varying degree, affect such material properties as thermal fatigue resistance and thermal stress cracking resistance. Due to technical and technological considerations, gray cast iron with flake graphite still has decisive advantages in using this material. The resistance to thermal fatigue in particular is decisive here. Additionally, by applying metallurgical procedures, e.g. inoculation of molten cast iron, we can control the precipitation of flake graphite and improve other mechanical properties. Bottom plates are flat, round, square



or rectangular castings with a thickness of up to 400 mm. In the Foundry of Krakodlew S.A. the bottom (and distance) plates can weigh up to 80 tons (Fig. 1a). In operation, plates are damaged as a result of cracks in places where the structural changes of the cast iron occur under the influence of high temperatures. In castings of plate weights (Fig. 1b), there are no problems resulting from the influence of high temperature, but there are problems with maintaining appropriate dimensional and weight accuracy.

The horizontal structure of the mold causes less problems than the vertical one in the production of large-size castings. On the other hand, the potential profits - the reduction of the time for machining and the reduction of the space occupied by the casting with the molds vertical ed to Krakodlew S.A. foundry in cooperation with the Faculty of Foundry Engineering of AGH, to conduct research in this field. Conducting the research was considered important because in the available literature one can find a small number of articles related to the large size and heavy castings and mainly focused on nodular cast iron [11-14]. There are even fewer articles regarding heavy castings produced in the vertical orientation of the mold [14].



Fig. 1. Examples of counterweight (a) and bottom plates (b) produced in Foundry Krakodlew S.A.

## 2. Research methodology

Three chemical compositions of high-quality modified cast iron were used for the tests. In the preliminary stage, they were

subjected to computer simulation with the ProCast software, in terms of shaping the structure and the formation of casting defects. Inoculated cast iron No. 1 has a hypoeutectic composition (Eutectic saturation  $S_c = 0.91$  and Carbon Equivalent  $CE = 3.93$ ), other cast irons No. 2 and 3 included in Table 1 have a eutectic composition.

Table 1.

The tested chemical compositions with the ProCast program

No	1	2	3
C, % mass	3.40	3.70	3.70
Si, % mass	1.66	1.70	2.00
Mn, % ass	0.61	0.61	0.61
Cr, % mass	0.08	0.08	0.08
Cu, % mass	0.03	0.03	0.03
Ni, % mass	0.02	0.02	0.02
S, % mass	0.04	0.04	0.04
P, % mass	0.10	0.10	0.10
$S_c$	<b>0.91</b>	<b>0.99</b>	<b>1.02</b>
CE	<b>3.93</b>	<b>4.25</b>	<b>4.33</b>
Austenite ( $T_\gamma$ ) and graphite ( $T_{gr}$ ) crystallization start temperature, °C			
$T_\gamma$	1208.5	1178.2	1172.4
$T_{gr}$	1165.1	1166.6	1169.7

The changes in the density of the analyzed chemical compositions of cast iron as a function of temperature are shown in Fig. 2.

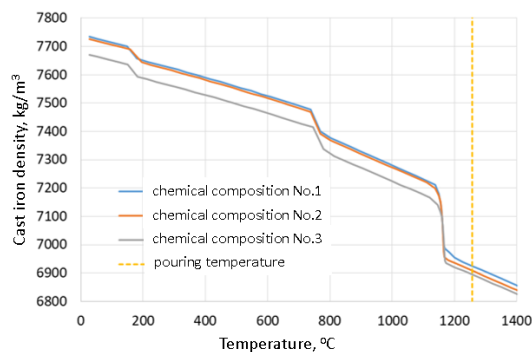


Fig. 2. Change of cast iron density with temperature change (results of calculations for the state of thermodynamic equilibrium, made using the CompuTherm Database)

Fig. 3-5 shows the shaping process of a 600 x 600 plate casting, 200 mm thick, poured vertically in a casting mold. The simulation results show that for the chemical compositions of the inoculated cast iron (shown in Table 1), the formation of a closed shrinkage cavity is observed. The smallest cavity is observed in the case of cast iron with chemical composition No. 3. In order to remove this type of defect (shrinkage cavity), it is necessary to develop a molding technology with an appropriate riser and an appropriate cast iron inoculation procedure. A micro model was used in the computer simulation (pouring temperature 1257 °C) to forecast the crystallization process (Fig. 3 – 5). This means that during crystallization, cast iron follows the path of non-equilibrium states. The actual changes in the density of cast iron are influenced by the deviation from the equilibrium state, i.e. both the nucleation rate of

the primary austenite grains and the "austenite-graphite" eutectic, and the migration speed of the "liquid-solid phase" interface during crystallization.

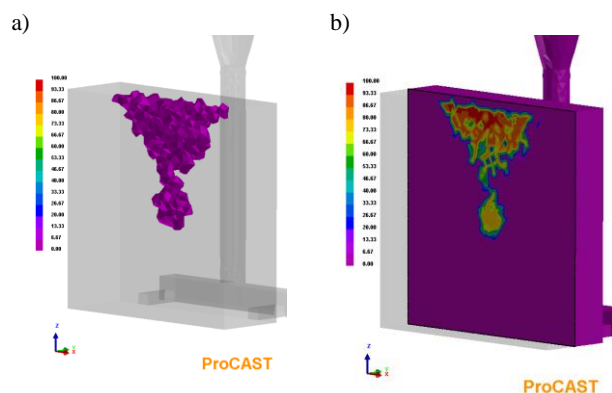


Fig. 3. Shrinkage defects in an inoculated cast iron casting, chemical composition No. 1: a) area of occurrence of shrinkage defects over 1% vol.; b) a cross-section through the center of the plate

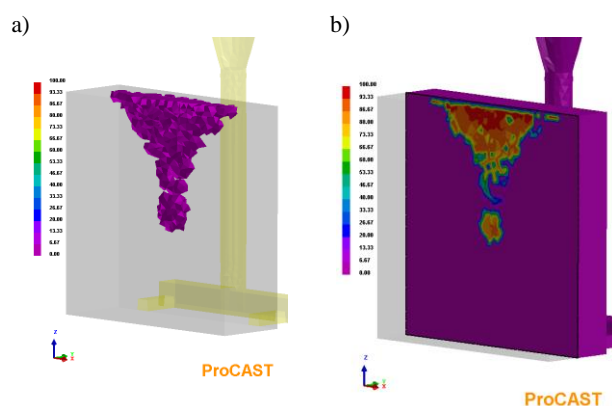


Fig. 4. Shrinkage defects in an inoculated cast iron casting, chemical composition No. 2: a) area of occurrence of shrinkage defects over 1% vol.; b) a cross-section through the center of the plate

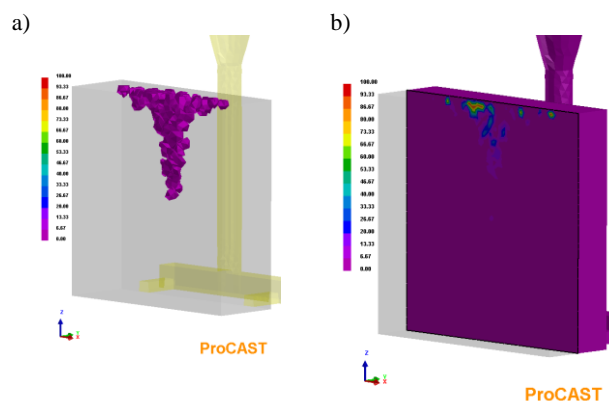


Fig. 5. Shrinkage defects in an inoculated cast iron casting, chemical composition No. 3: a) area of occurrence of shrinkage defects over 1% vol.; b) a cross-section through the center of the plate

In the next stage of the research, it was decided to analyze the gray cast iron modification procedure in laboratory conditions.

The melting was carried out in semi-industrial conditions in the experimental foundry at the Faculty of Foundry of the AGH University of Science and Technology. In the crucible of the medium-frequency induction furnace, the charge material (chemical composition of cast iron No. 3 in Table 1) was melted. The weight of the molten metal was 12 kg

After overheating to 1500 °C, the molten metal was held for 3 minutes and then the temperature was lowered to 1400 °C. At this temperature, the inoculation procedure was carried out using a different type of inoculant the assumed amount in relation to the mass of molten metal and modification of the original structure (austenite dendrite grains) with a steel bell weighing 100 g. The inoculation process was supposed to simulate the inoculation in the ladle in cored wire process. Due to the small amount of metal, it was carried out in a crucible in the furnace. After the bell and the inoculant dissolved in the molten metal, the crucible was removed from the furnace and transferred to the pouring station.

Standard shafts with a diameter of  $\phi 30 \times 270$  mm were cast.

### 3. Results

The chemical composition given by the manufacturer or distributor was as follows (Table 2):

Table 2.

The results of quantitative metallographic tests after using the Superseed inoculant

Inoculant /granulat.	Si	Ca	Al	Ba	Zr	Sr
Inolate	70-77	0.8-1.5	0.8-1.5	1.5-2.5		
Superseed	73-78	Max. 0.1	Max. 0.1			0.6-1.0
Zircinoc	73-78	2-2.5	1-1.5		1.3-1.8	
Fe - balance						
Granulation: Inolate – 0.2-0.7mm, Superseed and Zircinoc 2-5mm						

### 3.1 Superseed inoculant

Fig. 6, Table 3 and 4 shows the microstructures in the tested castings. During the melting, 0.35 of the Superseed inoculant was used.

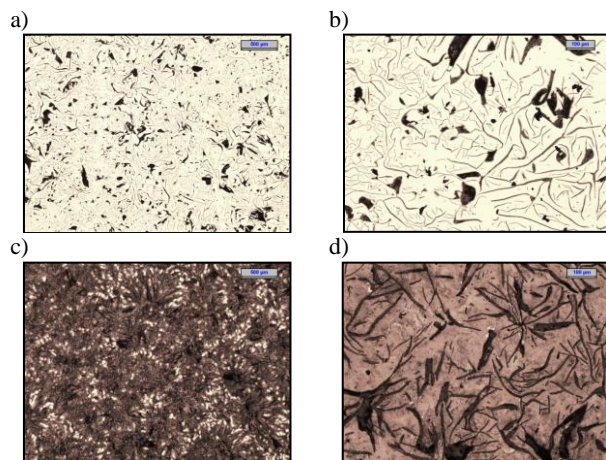


Fig. 6. The microstructure of cast iron after Superseed inoculation: non etched - a,b); etched: Stead's reagent - c), nital - d); magnification: 25x - a,c); 100x - b,d)

Table 3.

The results of quantitative metallographic tests after using the Superseed inoculant.

$N_A$ , $cm^{-2}$	A, %	B, %	D, %
324	40	30	30
	A - $L_{max}$	B - $L_{max}$	D - $L_{max}$
	376	672	98

$N_A$  – number of eutectic grains,

% A, B, C - percentage of the different types of graphite distribution,

$L_{max}$  - maximum dimensions of graphite,  $\mu m$

The results of the analysis of the chemical composition by the spectral method are shown in Table 3, and the carbon and sulfur content by the combustion method of the sample in the Horiba Emia 8200-B apparatus was as follows: C = 3.83% and S = 0.06%.

Table 4.

The results of the analysis of the chemical composition of the inoculated cast iron; spectral method - FECAIR

C	P	S	Si	Mn	Ni	Cr	Fe
3.73	0.02	0.06	2.05	0.70	0.05	0.17	res.

### 3.2. Zircinoc inoculant

Fig. 7, Table 5 and 6 shows the microstructures in the tested castings. During the melting, 0.35 of Zircinoc inoculant was used.

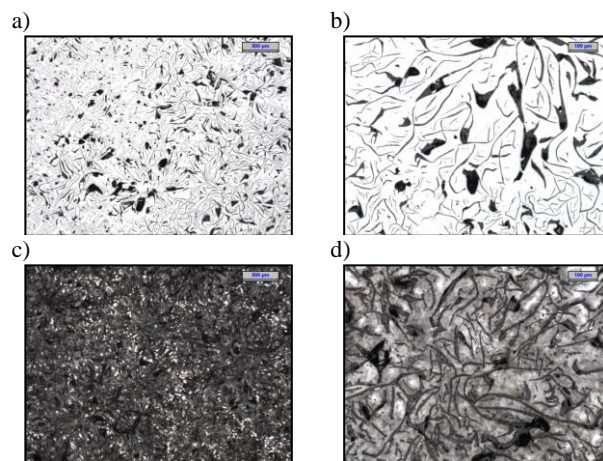


Fig. 7. The microstructure of cast iron after Zircinoc inoculation: non etched - a,b); etched: Stead's reagent - c), nital - d); magnification: 25x - a,c); 100x - b,d)

Table 5.

The results of quantitative metallographic tests after using the Zircinoc inoculant

$N_A$ , $cm^{-2}$	A, %	B, %	D, %
283	73	20	7
	A - $L_{max}$	B - $L_{max}$	D - $L_{max}$
	386	569	90

$N_A$  – number of eutectic grains,

% A, B, C - percentage of the different types of graphite distribution,

$L_{max}$  - maximum dimensions of graphite,  $\mu m$

The results of the analysis of the chemical composition by the spectral method are shown in Table 5, and the carbon and sulfur content by the combustion method of the sample in the Horiba Emia 8200-B apparatus was as follows: C = 3.76% and S = 0.064%.

Table 6.

The results of the analysis of the chemical composition of the inoculated cast iron; spectral method - Fecair

C	P	S	Si	Mn	Ni	Cr	Fe
3.64	0.04	0.06	2.09	0.60	0.05	0.23	res.

### 3.3. Inolate inoculant

Fig. 8, Table 7 and 8 shows the microstructures in the tested castings. During the melting, 0.35 of the Inolate inoculant was used.

The results of the analysis of the chemical composition by the spectral method are shown in Table 7, and the carbon and sulfur content by the combustion method of the sample in the Horiba Emia 8200-B apparatus was as follows: C = 3.90% and S = 0.064%.

Table 7.

The results of quantitative metallographic tests after using the Inolate inoculant

$N_A$ , cm <sup>2</sup>	A, %	B, %	D, %
357	55	15	30
	A - $L_{max}$	B - $L_{max}$	D - $L_{max}$
	367	724	67

$N_A$  – number of eutectic grains,

% A, B, C - percentage of the different types of graphite distribution,

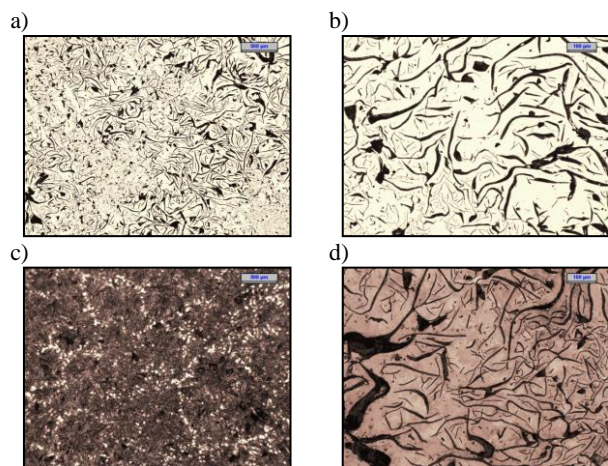


Fig. 8. The microstructure of cast iron after Inolate inoculation: non etched - a,b); etched: Stead's reagent - c), nital - d); magnification: 25x - a,c); 100x - b,d)

Table 8.

The results of the analysis of the chemical composition of the inoculated cast iron; spectral method - Fecair

C	P	S	Si	Mn	Ni	Cr	Fe
3.72	0.02	0.06	1.98	0.68	0.05	0.18	res.

The obtained supercooling degree values obtained during the tests are presented in Table 9.

Table 9.

The obtained degree of supercooling depending on the inoculation used

Inoculant	The degree of supercooling, °C
Superssed	18.27
Zircinoc	15.83
Inolate	18.63

## 4. Conclusions

- The results of the experimental tests show that the overheating temperature of the metal at 1500 °C for three minutes gives good results in terms of graphite homogeneity. Such overheating of the metal contributes to the physicochemical state of the molten alloy, ensuring a more

favorable microstructure of the graphite flakes, especially its proper distribution and size.

- Experimental studies show that the inoculant with fine granulation requires dosing that prevents its oxidation on the surface of the molten metal. This is the case when it is introduced, for example, on the surface of the molten melt in the crucible. For this purpose, a "steel bell" was used in which the inoculant was dosed. The use of the "steel bell" essentially weakens the inoculation effect (a smaller number of graphite eutectic grains), however, it affects the primary crystallization of austenite.
- The research shows that the use of the inoculation method with the use of a steel bell contributed to an increase in the homogeneity of the cast iron microstructure in terms of the graphite precipitation characteristics.
- The use of the Zircinoc inoculant caused a significant decrease in the volume fraction of D-type graphite, even to the level of 3% in standard cast shafts. At the same time, the degree of undercooling has the lowest value.

## Acknowledgements

The publication was created during the implementation of the RPMP.01.02.01-12-0055 / 18 project at Krakodlew S.A. financed by the Regional Operational Program of the Lesser Poland Voivodeship.

## References

- Benedetti, M., Torresani, E., Fontanari, V. & Lusuardi, D. (2017). Fatigue and fracture resistance of heavy-section ferritic ductile cast iron. *Metals*. 7(3), 88.
- Dorula, J., Kopyciński, D., Guzik, E., Szczęsny, A. & Gurgul, D. (2021). The influence of undercooling  $\Delta T$  on the structure and tensile strength of grey cast iron. *Materials*. 14(21), 6682.
- Wang, Q., Cheng, G. & Hou, Y. (2020). Effect of titanium addition on as-cast structure and high-temperature tensile property of 20Cr-8Ni stainless steel for heavy castings. *Metals*. 10(4), 529.
- Wang, Q., Chen, S. & Rong, L. (2020).  $\delta$ -Ferrite formation and its effect on the mechanical properties of heavy-section AISI 316 stainless steel casting. *Metallurgical and Materials Transactions A*. 51, 2998-3008.
- Kalandyk, B., Zapala, R., Sobula, S., Górný, M. & Boroń, Ł. (2014). Characteristics of low nickel ferritic-austenitic corrosion resistant cast steel. *Metallurgija-Metallurgy*. 53(4), 613-616.
- Kalandyk, B. & Zapala, R. (2013). Effect of high-manganese cast steel strain hardening on the abrasion wear resistance in a mixture of SiC and water. *Archives of Foundry Engineering*. 13(4), 63-66.
- Tećca, G. & Zapala, R. (2018). Changes in impact strength and abrasive wear resistance of cast high manganese steel due to the formation of primary titanium carbides. *Archives of Foundry Engineering*. 18(1), 119-122.

- [8] Tęcza, G. & Garbacz-Klempka, A. (2016). Microstructure of cast high-manganese steel containing titanium. *Archives of Foundry Engineering*. 16(4), 163-168.
- [9] Celis, M., Domengès, B., Hug, E. & Lacaze, J. (2018). Analysis of nuclei in a heavy-section nodular iron casting. *Materials Science Forum*. 925, 173-180.
- [10] Kopyciński, D., Siekaniec, D., Szczęsny, A., Sokolnicki, M. & Nowak, A. (2016). The Althoff-Radtke test adapter for high chromium cast iron. *Archives of Foundry Engineering*. 16(4), 74-77.
- [11] Szczęsny, A., Kopyciński, D., Guzik, E. Soból, G., Piotrowski, K., Bednarczyk, P. & Paul, W. (2020). Shaping of ductile cast iron dedicated for slag ladle. *Acta Metallurgica Slovaca*. 26, 74-77. <https://doi.org/10.36547/ams.26.2.312>
- [12] Mourad, M.M. & El-Hadad, S. (2015). Effect of processing parameters on the mechanical properties of heavy section ductile iron. *Journal of Metallurgy*. 2015, 1-11.
- [13] Foglio, E., Gelfi, M., Pola, A. & Lusuardi, D. (2017). Effect of shrinkage porosity and degenerated graphite on fatigue crack initiation in ductile cast iron. *Key Engineering Materials*. 754, 95-98.
- [14] Kavicka, F., Sekanina, B., Stetina, J., Stransky, K., Gontarev, V. & Dobrovska, J. (2009). Numerical optimization of the method of cooling of a massive casting of ductile cast-iron. *Materials and Technology*. 43, 73-78.